

QUANTITATIVE ANALYSIS OF LAND MULTIPLE REFLECTED REFRACTIONS

TONG LIN¹, CHAOBIN GUO² and SONGQI PAN¹

¹ *Department of Gas Geology, Research Institute of Petroleum Exploration and Development, PetroChina, Langfang 065007, P.R. China.*

² *Sinochem Petroleum Exploration & Production Co., Ltd., Beijing 100031, P.R. China.
cbguo1971@163.com*

(Received February 24, 2018; revised version accepted January 31, 2019)

ABSTRACT

Lin, T., Guo, C.B. and Pan, S.Q., 2019. Quantitative analysis of land multiple reflected refractions. *Journal of Seismic Exploration*, 28: 163-173.

Multiple reflected refractions are an important wave phenomenon in shallow layer, predominantly in karst mountain area, or piedmont tectonic belt. In this paper, we discover the actual the actual propagation path of multiple reflected refractions, and discuss the characteristics of multiple reflected refractions by math formula derivation, including the kinematic and dynamic issues. The results show that the study of multiple reflected refractions is of great significance to understand seismic refractions.

KEY WORDS: multiple reflected refractions, propagation path, kinematic and dynamic characteristics.

INTRODUCTION

The study of head waves originally began in the early 20th century. Jeffreys (1926) was the first to deduce the formula for describing head waves, and Muskat (1933) deduced the approximate expression of head waves by the Sommerfeld integral. Up to 1955, most of the research was based on the integral method. The most comprehensive theory on head waves was proposed by Cagniard (1962), with complex mathematics and difficult integral solution. Alekseyev (1958) firstly applied the ray theory to formulate an expression of head waves at the interface of solid media. In addition, Cerveny and Ravinda (1971) published their monograph on head waves, discussing most theoretical and practical problems of head waves by the ray method.

With seismic exploration hotspots turned to the uplift of the basin, the mountain carbonate area and piedmont tectonic belt area, multiple reflected refractions have become a key issue to seismic data acquisition, processing and interpretation (Yilmaz, 2001; Hill, 1972), whether to improve the signal-to-noise ratio of the seismic data or obtain the related near-surface information from the multiple refractions (Domzalski, 1956; Bennett, 1999; Rao et al., 2007).

In this paper, we will find out the actual propagation path of multiple reflected refractions, and analyze the kinematic and dynamic characteristics to understand this important wave phenomenon.

THE PROBLEM OF MULTIPLE REFLECTED REFRACTIONS

Multiple reflected refractions exist widely in the seismic records from karst mountain area, or piedmont tectonic belt. Fig. 1 depicts the multiple reflected refractions in original 2D and 3D shot records. The left figure is a 2D shot record from karst mountain area in Sichuan basin of south China, where five sets of parallel refractions inside the red rectangular have similar characteristics in terms of apparent velocity, frequency band and phase, caused by an underground gravel layer. The right is a 3D shot record lasting to 3100 ms in a karst mountain area, and the parallel refractions in the red rectangular have the same apparent velocity as the head wave, where there is a strong interface between low velocity mudstone and high velocity limestone detected by the LVL and the uphole methods (Zhu et al., 2008; Palm, 2001; Chen, 1999). These parallel refractions could seriously affect the reflection waves, which may make the resolution of the seismic data lower.

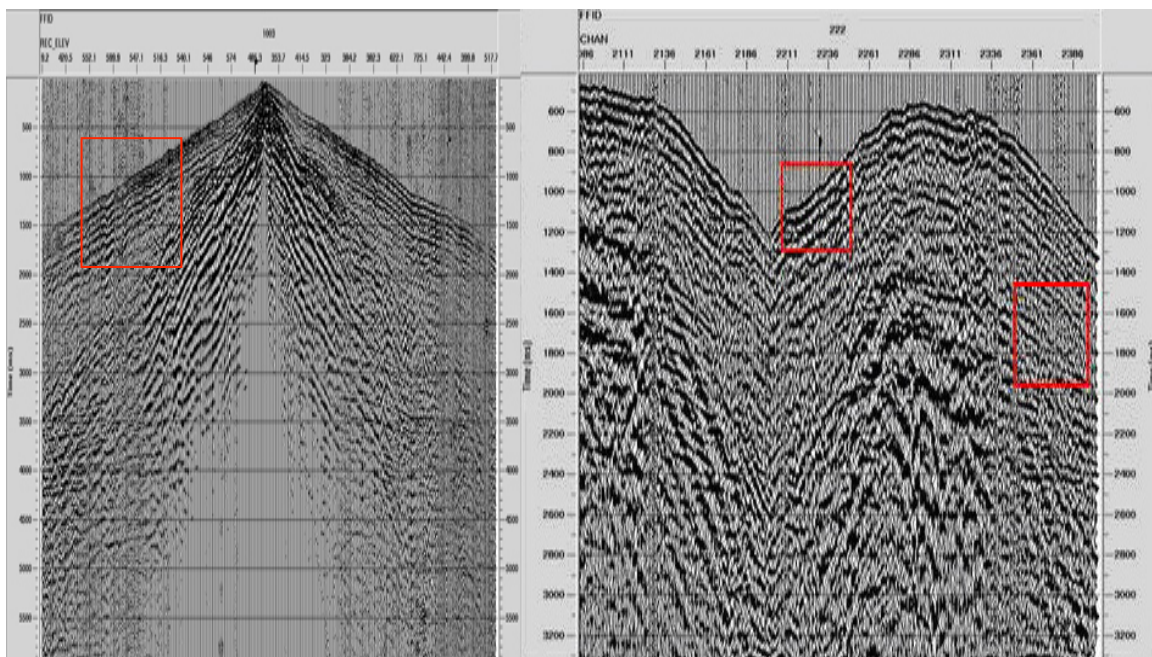


Fig. 1. Original shot records with multiple reflected refractions.

The events should be defined as multiple reflected refractions in the red rectangular for they have the same apparent velocity, frequency band and phase as the head wave. When the incidence angle of the multi-reflection wave within the upper low-velocity layer is equal to the critical angle, slide waves are formed along the top surface of the high-velocity layer, thereby developing a series of multiple reflected refractions. Since multiple reflected refractions and first-arrival refracted waves propagate along the same interface, their apparent velocities are equal.

THE CHARACTERISTICS OF MULTIPLE REFLECTED REFRACTIONS

The propagation path of multiple reflected refractions

It is easy to understand that the prerequisite for multiple reflected refractions generated is that the interface between an overlying low velocity layer and the underlying high velocity layer should be nearly parallel (Aki and Richards, 2002; Kennett, 1983). Meanwhile, there is an ambiguity in the propagation path of multiple reflected refractions. Fig. 2 displays two possible propagation paths of multiple reflected refractions. Path I indicates that the n -th refraction waves are generated after the incidental waves are reflected $(n - 1)$ times, whereas wave path II indicates that the refraction waves are reflected $(n - 1)$ times after the refraction waves are first generated. For a given offset, both propagation paths will take the same travel time, but with different amplitudes, which means that both paths have the same kinematic characteristic, but different dynamic characteristic. Hence the problem arises of which path represents the real one.

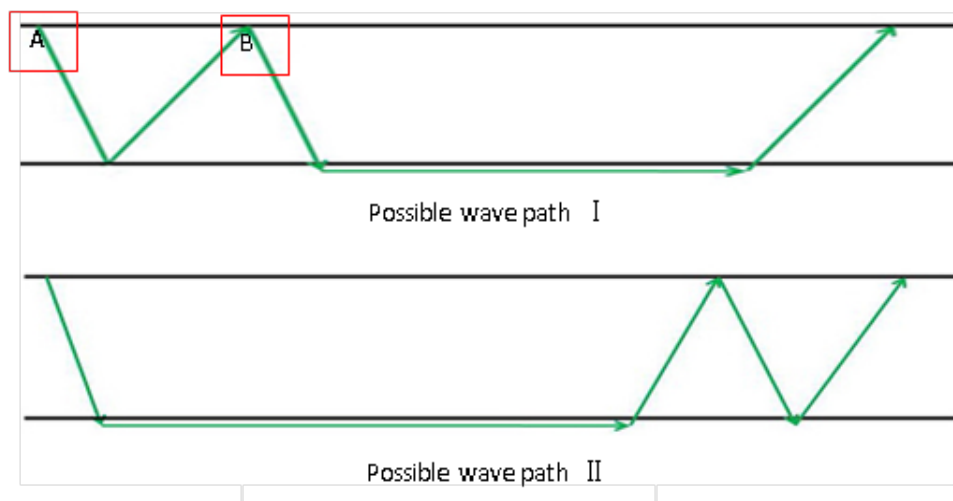


Fig. 2. Possible wave paths of multiple refractions.

In order to obtain clear information about the generation of multiple refractions, we have built two forward modeling by the spectral element method (Komatitsch and Tromp, 1999; Huang et al., 2010; Segers and

Verdonck, 2000). One model is an elastic half-space model and the other is a low velocity waveguide model, both with 1000×300 grid points and a grid size of 0.5 meter. The elastic parameters of the velocity models, including compressional and shear velocities as well as density, are shown in Table 1.

Table 1. Velocity model used to calculate the multiple refractions.

<i>Model</i>	V_p	V_s	<i>Density</i>
<i>number</i>	(m/s)	(m/s)	(g/cm ³)
M_I	0.90	0.52	2.0
M_II	2.20	1.28	2.25

Each model ran for 10000 time steps at 0.00005 seconds per step for a total calculation time of 0.5 seconds. The source time function used is the Ricker wavelet with a dominant frequency of 145 Hz. The point source A in Fig. 2 is located 80 meters from the left side and at a depth of 10 meters from the surface of the model. Results for both models are shown in Fig. 3 which presents the vertical displacement component. The half space time series (Fig. 3a) reveals the amplitude decreasing with the increase in offset from the source at 80 meters. While the presence of the low-velocity wave guide (Fig. 3b) has a dramatic effect on the displacement time series on condition that the energy of the wave field is trapped in the wave guide. As a result, multiple refractions can be detected and the energy of the multiple refractions is much higher than for the direct signal (Fig. 3a). Hence, we can confirm that path I (Fig. 2) is the real one for the generation of multiple refractions while, based on the results of forward modeling (Fig. 3). Path I indicates that the incident waves are reflected several times initially near the source and generate refractions in the wave guide layer.

The kinematic characteristics of multiple reflected refractions

Fig. 4 shows the propagation of multiple reflected refractions in 3D. On the left, the bottom surface is the top of the downlap layer with high velocity v_2 and thickness h_2 , while free surface as the top surface, and that between them is an overlying layer with low velocity v_1 and thickness h_1 . The point O, line AB and OA, respectively, denote the source point location, the reception spread and the minimum offset distance for the reflection refraction generation. In addition, the critical angle, the length of the lines AB and OA are labeled as θ , x and d , respectively. After shooting at the source point, there will be refraction waves first on the top of high-velocity layer. Then after these sliding waves are reflected at the free surface, multiple reflected refractions will appear when the incident angle is equal to the critical angle. $OMC'M'B$ is the ray path of reflection waves received at point B, with the incidence angle β and transmission angle γ .

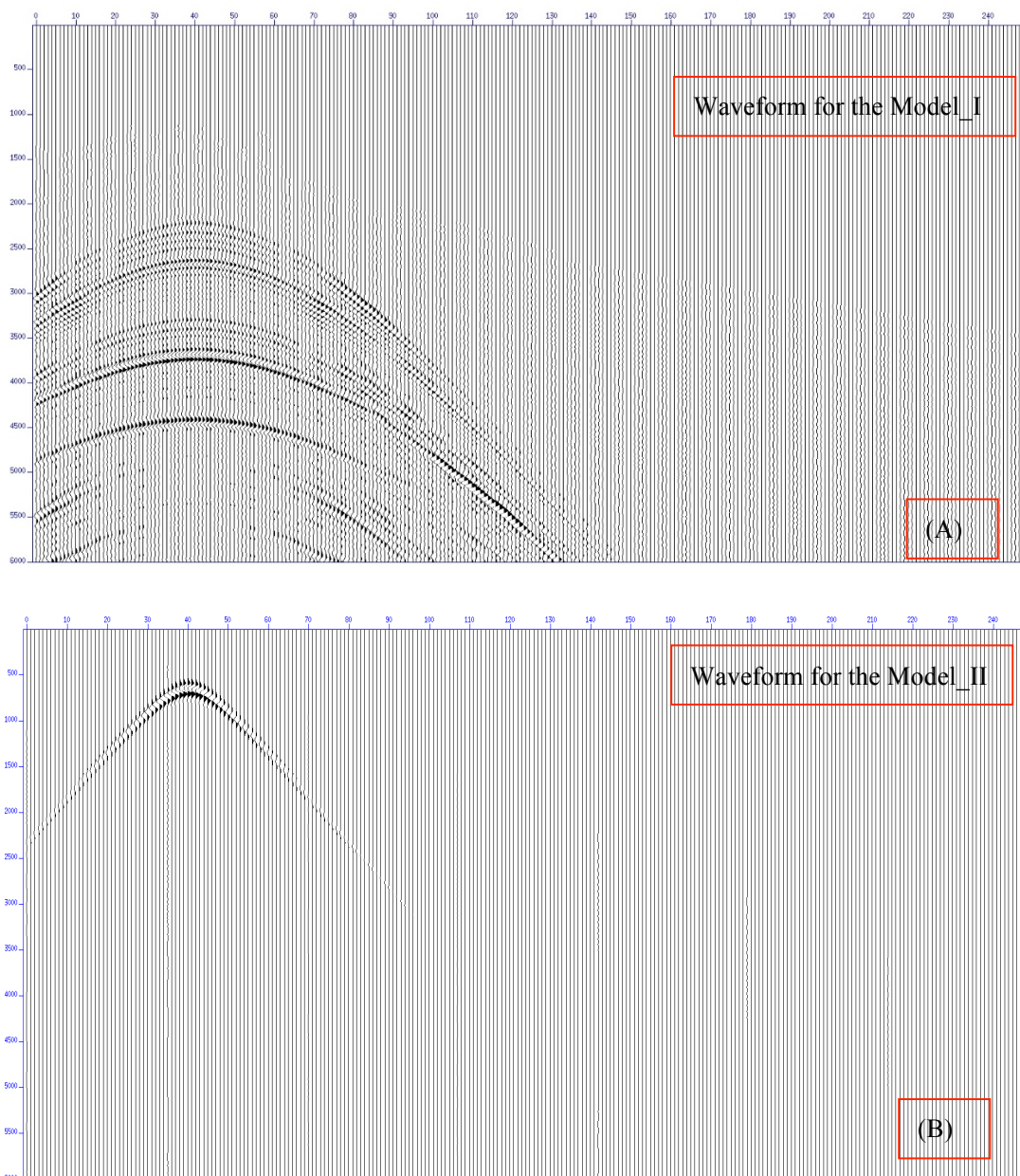


Fig. 3. The vertical component of the synthetic waveform for the Model I (A) and Model II (B) in Table 1.

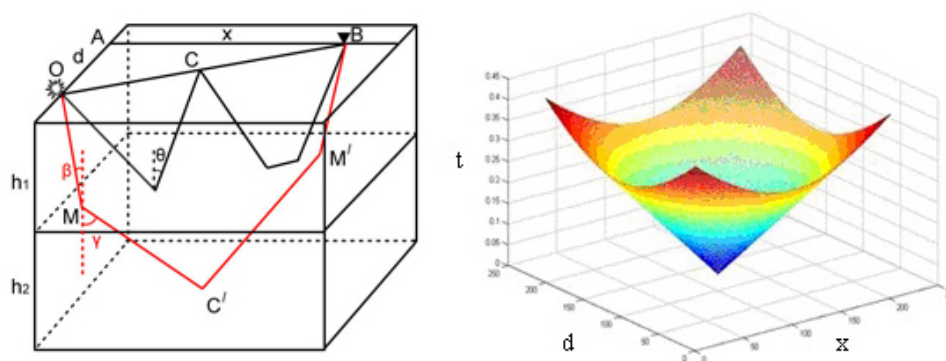


Fig. 4. Ray path of multiple refractions and its hodograph.

According to the time–distance curve formula of refractions, in the case of a 2D horizontal interface:

$$t = \frac{x}{v_2} + \frac{2h_1 \cos \theta}{v_1} \quad , \quad (1)$$

(Lu, 2001; Palmer, 2006; Piip, 2001). We could derive the equation of secondary reflected refractions in the 3D case (Fig. 4) as:

$$t = \frac{4h_1}{v_1 \cos \theta} + \frac{\sqrt{x^2+d^2}-4h_1 \tan \theta}{v_2} = \frac{\sqrt{x^2+d^2}}{v_2} + \frac{4h_1 \cos \theta}{v_1} \quad , \quad (2)$$

Then the following expression can be rewritten from eq. (2) as:

$$\frac{(v_2 t - 4h_1 \cot \theta)^2}{d^2} - \frac{x^2}{d^2} = 1 \quad . \quad (3)$$

The travel time t in eq. (3) satisfies the hyperbolic laws, shown in Fig. 4 as a circular conical surface. Hence, we could derive the expression of the travel time of the n th reflected refraction in the same way:

$$\frac{(v_2 t - 2nh_1 \cot \theta)^2}{d^2} - \frac{x^2}{d^2} = 1 \quad . \quad (4)$$

For the horizontal layered media, according to the time–distance curve formula of 2D m -th horizontal interface (Lu, 2001):

$$t = \frac{x}{v_m} + 2 \sum_{k=0}^{m-1} \frac{h_k \cos \theta_{km}}{v_k} \quad (5)$$

The v_m denotes the velocity of the m -th horizontal interface, and h_k , v_k and θ_{km} denote the thickness, velocity and angle of incidence of the k -th layer, respectively. In addition, the time–distance curve formula of the m -th horizontal interface could be derived as:

$$\frac{(v_m t - 2 \sum_{k=0}^{m-2} h_k \cot \theta_{km} - 2(n+1)h_{m-1} \cot \theta_{m-1m})^2}{d^2} - \frac{x^2}{d^2} = 1 \quad (6)$$

In eq. (6), n denotes the n -th refraction, and the term $2 \sum_{k=0}^{m-2} h_k \cot \theta_{km}$ is a constant. Eq. (6) suggests that the travel time, t , with d , x argument also satisfy the hyperbolic laws.

A similar equation for dipping interfaces also could be derived, but due to the limitation of stratigraphic dip angle and critical angle, there would be not many times of refraction waves and t no need to go into further details.

The dynamic characteristics of multiple reflected refractions

Based on both the ray approximation method and seismic wave dynamic theory, the existence of refraction has been verified, and some researchers have studied the dynamic characteristics of the refractions in detail (Cerveny, 1971; Sheriff, 1995; Fuchs and Müller, 1971). However, since multiple reflected refractions are related to reflection waves, it is necessary to study and quantitatively analyze its dynamic characteristics (Franco, 2005).

For a harmonic source, the emitted spherical harmonic wave's potential:

$$\varphi^0 = \frac{1}{-ikR_0} e^{i\omega(t-R_0/v_1)} \quad , \quad (7)$$

R_0 denotes the distance to the sources, and k is the wave number with $k = \omega/v_1$, where ω is the frequency of the source. According to Fig. 4, the displacement of the reflection wave related to the refraction interface could be expressed as:

$$W^*(m) = \frac{1}{\sqrt{x^2+d^2+4h_1^2}} e^{i\omega(t-\tau)} R_j^0 R_j^1 N^*(m) \quad , \quad (8)$$

(Brekhovskikh, 1960). In eq. (8), m and x denote the receiver point and offset, respectively, $N^*(m)$ denotes the vector of displacement, R_j^0 is the reflection coefficient of a free surface, R_j^1 is the reflection coefficient of the refraction interface, and R_j^0, R_j^1 could be considered as constants, but when reflections occur at the critical point, the reflection coefficient should be calculated accurately. When the angle of incidence is equal to the critical angle θ , the reflection coefficient by Cerveny (1971) could be modified to:

$$R_j^1 = B(\sin\theta) - \frac{i}{\sin\theta} \Gamma_k \left(\frac{2\sin\theta^3}{2\pi f \sqrt{x^2+d^2}} \right)^{1/4} \sqrt{2\cos\theta} g(0) \quad , \quad (9)$$

$B(\sin\theta)$ is related with the medium's elastic parameter and $B(\sin\theta) < 1$, with

$$g(0) = \frac{1}{\sqrt{\pi}} \int_{-\infty}^{+\infty} (-xe^{-i\pi/4})^{1/2} e^{-x^2} dx \quad . \quad (10)$$

For the reflection related to the horizontal layered media, the displacement equation of the head wave by Cerveny (1971) as:

$$W^{mnp}(m) = \frac{v_n \Gamma_{mnp} \tan \theta}{i \omega x^{1/2} (x - x_m)^{3/2}} e^{i\omega(t - \tau_{mnp})} N^*(m) \quad , \quad (11)$$

where x_m denotes the critical distance. For multiple refraction, if the incident waves with the critical angle θ are regarded as new irritation sources, the potential of the n-th incident wave could be expressed as:

$$\Phi = \frac{1}{2nh_1 / \cos \theta} (nR^1_j)(nR^0_j) e^{i\omega(t - \tau)} \quad , \quad (12)$$

where the n-th multiple refraction could be regarded as the first refraction by the new source. By reference to eq. (11), the displacement of the n-th refraction at point B outside of the region of interference, can be deduced as:

$$W(m) = \frac{\frac{1}{2nh_1 / \cos \theta} (nR^1_j)(nR^0_j) v_k \Gamma_k \tan \theta}{i \omega (\sqrt{x^2 + d^2} - 2nh_1 \tan \theta)^{1/2} (\sqrt{x^2 + d^2} - 2(n+1)h_1 \tan \theta)^{3/2}} e^{i\omega(t - \tau)} N^*(m) \quad , \quad (13)$$

where Γ_k is the head wave coefficient, and v_k being the velocity of refraction. The influences of recording spread length and times of refraction on displacement $W(m)$ embody in the denominator. If the thickness of the low-velocity layer h_1 is constant, we can make the following assumption:

$$P = n(\sqrt{x^2 + d^2} - 2nh_1 \tan \theta)^{-1/2} (\sqrt{x^2 + d^2} - 2(n+1)h_1 \tan \theta)^{-3/2} \quad . \quad (14)$$

In eq. (13), the trend of P is in accordance with that of the amplitude of the refraction displacement at any receiver points outside of the interference region. If we set the critical distance for 50 m, with x_m being the critical distance, and the offset $\sqrt{x^2 + d^2}$ labeled as L, the amplitude trend of the multiple refraction as a dependent variable of the offset L and times N would be shown in Fig. 5. The figure shows the amplitude of the multiple refraction decreases with the increasing offset. In addition, the amplitude of the 3rd refraction is larger than that of the 2nd refraction.

In general, multiple refraction are thought to be weaker and weaker, so why does this contrasting phenomenon occur?

When the shot records contain multiple refractions, for a certain receiver with a given offset in eq. (13), the amplitude ration of the (n+1)-th refraction to the n-th refraction can be written as:

$$\eta = \frac{A_{n+1}}{A_n} = \frac{W_{n+1}}{W_n} = \frac{n+1}{n} \frac{(\sqrt{x^2+d^2-2nh_1\tan\theta})^{1/2} (\sqrt{x^2+d^2-2(n+1)h_1\tan\theta})}{(\sqrt{x^2+d^2-2(n+2)h_1\tan\theta})^{3/2}} \quad (15)$$

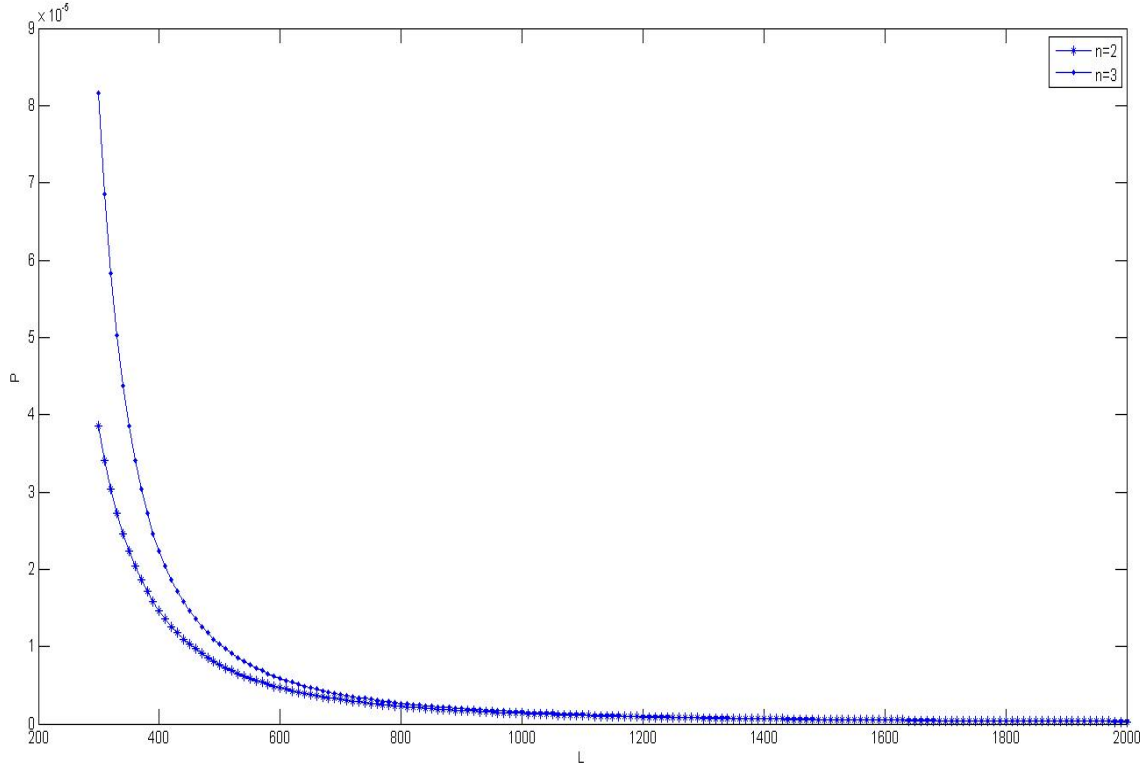


Fig. 5 . Tendency of refraction amplitude vs. L and N.

In eq. (15), defining $f(n)$ as:

$$f(n) = \sqrt{x^2 + d^2 - 2nh_1\tan\theta} \quad , \quad (16)$$

as $f(n)$ is a monotone decreasing function of argument n, also $\frac{n+1}{n} > 1$, so

for eq. (15)

$$\eta > 1 \quad , \quad (17)$$

eq. (17) indicates that the amplitude of the (n+1)-th refraction is larger than that of the n-th refraction for a given offset. In theory, the n-th refraction propagates along more ray paths than the (n+1)-th refraction waves, so that

the n -th refraction waves diverge more refraction energy, which is the geophysical meaning of eq. (17).

CONCLUSION

Multiple reflected refractions in complex territory such as karst mountain area, or piedmont tectonic belt have been a key wave phenomenon by its wide existence and negative influence on the reflection waves.

We have summarized two possible propagation paths of multiple refracted reflection through the deduction of propagation path, and two possible paths are verified by the spectral element forward modeling method based on a half-space model and a wave guide model. Therefore, the actual propagation path is verified by the results of modeling, which means that the incident waves are reflected several times initially near the source and generate refractions in the wave guide layer.

The original study is to understand the kinematics and dynamic characteristics of multiple reflected refractions by stack math formulation derivation. Based on the analysis of these characteristics, we have obtained two meaningful results: (1) The travel time of multiple reflected refractions satisfies the hyperbolic laws; (2) the amplitude of the $(n+1)$ -th refraction is larger than that of the n -th refraction with a given offset.

ACKNOWLEDGEMENTS

This research was funded by the National Nature Science Foundation of China (SN: 40974073), the National 863 Project (SN: 2007AA060504), and the Young Scholar Foundation of the China University of Petroleum (SN:10CX04001A).

REFERENCES

- Aki, K. and Richards, P.G., 2002, Quantitative Seismology. University Science Books, Sausalito, CA.
- Alekseyev, A.S. and Gel'chinskiy, B.Y., 1958. Determination of the intensity of head waves in the theory of elasticity by the ray method. Doklady Akad. Nauk SSSR, 118: 661-664.
- Bennett, G., 1999. 3D seismic refraction for deep exploration targets: The Leading Edge, 18: 186-191.
- Brekhovskikh, 1960. Layered Media. Academic Press Inc., New York.
- Cagniard, L., 1962. Reflection and Refraction of Progressive Seismic Waves. McGraw-Hill, New York.
- Cerveny, V. and Ravindra R., 1971. Theory of Seismic Head Waves. Univ. of Toronto Press, Toronto.
- Chen, X.F., 1999. Seismogram synthesis in multi-layered half-space. Part I. Theoretical formulation. Earthq. Res. China, 13: 150-174.

- Domzalski, W., 1956. Some problems of shallow seismic refraction investigations. *Geophys. Prosp.*, 4: 140-166.
- Franco, R.D., 2005. Multi-refractor imaging with stacked refraction convolution section. *Geophys. Prosp.*, 53: 335-348.
- Fuchs, K. and Müller, G., 1971. Computation of synthetic seismograms with reflectivity method and comparison with observations. *Geophys. J. Roy. Astron. Soc.*, 23: 417-433.
- Hill, D., 1972. Velocity gradients and anelasticity from crustal body wave amplitudes. *J. Geophys. Res.*, 76: 3309-3325.
- Huang, J.P., Vanacore, E., Niu, F. and Levander, A., 2010. Mantle transition zone beneath the Caribbean-South American plate boundary and its tectonic implications. *Earth Planet. Sci. Lett.*, 289: 105-111.
- Jeffreys, J., 1926. On compressional waves in two superposed layers. *Proc. Cambridge Phil. Soc.*, 23.
- Kennett, B.L.N., 1983. *Seismic Wave Propagation in Stratified Media*. Cambridge University Press, Cambridge: 1-5.
- Komatitsch, D. and Tromp, J., 1999. Introduction to the spectral element method for three-dimensional seismic wave propagation, *Geophys. J. Internat.*, 139: 806-822.
- Lu, J.M., 2001. *Principles of Seismic Exploration*. Dong Ying: Express of China University of Petroleum, Beijing.
- Muskat, M., 1933. The theory of refraction shooting physics, 4: 14-28.
- Palmer, D., 2001. A new direction for shallow refraction seismology: integrating amplitudes and traveltimes with the refraction convolution section. *Geophys. Prosp.*, 49: 657-673.
- Palmer, D., 2006. Refraction traveltime and amplitude corrections for very near-surface inhomogeneities. *Geophys. Prosp.*, 54: 589-604.
- Piip, V.B., 2001. 2D inversion of refraction traveltime curves using homogeneous functions. *Geophysical Prospecting*, 49(4): 46-1482.
- Rao, V.V., Sain, K. and Krishna, V.G., 2007. Modelling and inversion of single-ended refraction data from the shot gathers of multifold deep seismic reflection profiling - an approach for deriving the shallow velocity structure. *Geophys. J. Internat.*, 169: 507-514.
- Segers, P. and Verdonck, P., 2000. Role of tapering in aortic wave reflection: hydraulic and mathematical model study. *J. Biomechan.*, 24: 33-43.
- Sheriff, R.E. and Geldart, L.P., 1995. *Exploration Seismology*. Cambridge University Press, Cambridge: 261-263.
- Yilmaz, O., 2001. *Data Analysis: Processing, Inversion, and Interpretation of Seismic Data*. SEG, Tulsa, OK.
- Zhu, X., 2008. Problems of seismic exploration for marine hydrocarbon reservoirs in southern China and some countermeasures. *Progr. Explor. Geophys.*, 31: 318-319.